TISSUE ENGINEERING: Part A
Volume 21, Numbers 7 and 8, 2015
Mary Ann Liebert, Inc.
DOI: 10.1089/ten.tea.2014.0297

Biocompatibility and Characterization of a Peptide Amphiphile Hydrogel for Applications in Peripheral Nerve Regeneration

Katie A. Black, PhD,[1,2] Brian F. Lin, PhD,[1] Emily A. Wonder, BA,[3] Seema S. Desai, BA,[1] Eun Ji Chung, PhD,[3] Bret D. Ulery, PhD,[3] Ravi S. Katari, BS,[3] and Matthew V. Tirrell, PhD[1–3]

Peripheral nerve injury is a debilitating condition for which new bioengineering solutions are needed. Autografting, the gold standard in treatment, involves sacrifice of a healthy nerve and results in loss of sensation or function at the donor site. One alternative solution to autografting is to use a nerve guide conduit designed to physically guide the nerve as it regenerates across the injury gap. Such conduits are effective for short gap injuries, but fail to surpass autografting in long gap injuries. One strategy to enhance regeneration inside conduits in long gap injuries is to fill the guide conduits with a hydrogel to mimic the native extracellular matrix found in peripheral nerves. In this work, a peptide amphiphile (PA)-based hydrogel was optimized for peripheral nerve repair. Hydrogels consisting of the PA C_{16}GSH were compared with a commercially available collagen gel. Schwann cells, a cell type important in the peripheral nerve regenerative cascade, were able to spread, proliferate, and migrate better on C_{16}GSH gels *in vitro* when compared with cells seeded on collagen gels. Moreover, C_{16}GSH gels were implanted subcutaneously in a murine model and were found to be biocompatible, degrade over time, and support angiogenesis without causing inflammation or a foreign body immune response. Taken together, these results help optimize and instruct the development of a new synthetic hydrogel as a luminal filler for conduit-mediated peripheral nerve repair.

Introduction

Peripheral nerve injury (PNI) is a debilitating condition, which affects 2.8% of trauma patients, and can result in lifelong disability.[1] Autografting, the current gold standard treatment for PNI, involves removal of a piece of a healthy sensory nerve from elsewhere in the body (often the sural nerve, a sensory nerve of the lower leg) and attachment to the severed nerve ends to guide regeneration.[2] Autografting is limited by availability of expendable donor nerves and results in a second injury with loss of sensation at the donor site.[3] To address the inherent limitations of autografting, nerve guide conduits have been developed as an alternative. Nerve guide conduits are traditionally hollow tubes that, when used to connect the two severed ends of a nerve injury, aid in neural repair by directing axons toward the distal stump and minimizing infiltration of scar tissue.[4] Conduits have been created from both natural and synthetic sources, and four conduits have been approved by the FDA for use in limited gap length injuries.[5,6] Nerve guides have shown comparable efficacy in 20–25 mm injuries, but are inferior to autografts in long gap injuries.[7,8]

To surpass the efficacy of autografts, especially in long gap repair, improvements must be made to the hollow tube design of current nerve guide conduits.[9,10] One strategy to enhance regeneration is to engineer internal structure into the hollow tube by adding internal channels, aligned fibers, or by filling with a soft material such as a hydrogel.[11] In designing a hydrogel to enhance peripheral nerve regrowth, the natural progression of regeneration must be considered. During the regeneration process, macrophages and fibroblasts first enter the injury space to remove debris and deposit an extracellular matrix framework, respectively. Schwann cells then detach from the proximal nerve to proliferate and migrate into the injury gap toward the distal nerve stump. Following the Schwann cells, new axons sprout from the severed proximal nerve stump and reconnect to the distal nerve stump, completing the regeneration process.[12] Thus, an ideal conduit gel

[1]Department of Bioengineering, University of California Berkeley, Berkeley, California.
[2]UC Berkeley—UCSF Graduate Program in Bioengineering, Berkeley, California.
[3]Institute for Molecular Engineering, University of Chicago, Chicago, Illinois.

filler should mimic the peripheral nerve environment and enhance the activity of regenerating Schwann cells. Collagen and laminin have both been investigated as potential luminal gel fillers for this application.[13–15] Although collagen gels have had some success, there are difficulties in precise control of the stiffness, and Type I collagen gels sourced from animals have been shown to produce a deleterious immune response in patients.[16]

Synthetically based hydrogels are ideal to allow precise control of mechanical and biochemical properties while avoiding potential negative immune responses. One type of material, the peptide amphiphile (PA), is an attractive material to fill this need based on its ease of synthesis, modular design, and self-assembly properties.[17] PAs are made by conjugating short peptide sequences to fatty acid tails. The hydrophilic (peptide) and hydrophobic (fatty acid tail) components of the PA cause them to self-assemble at low concentrations into spherical micelles, long worm-like micelles, or liposomes depending on the PA design.[18] Worm-like micelles, which are typically nanometers in diameter and microns in length, can entangle at a high concentration to form a viscoelastic hydrogel.[19] PAs have been used in a variety of biomedical applications, including imaging,[20,21] biomineralization,[22,23] drug delivery,[24,25] gene delivery,[26,27] immunotherapy,[28] cancer therapeutics,[29,30] and regenerative medicine.[31] In particular, PAs designed to form worm-like micelles that give rise to hydrogels have shown promise in the area of neural-based tissue engineering, such as spinal cord injury[32,33] and cavernous nerve injury.[34] Based on this encouraging evidence, it was suggested in a recent review that PA gels would be well suited for the application of a filler material for PNI.[17]

One particular PA, developed in our laboratory, termed C_{16}GSH (Fig. 1), has been shown to have favorable material properties and biocompatibility. C_{16}GSH hydrogels respond to pH changes due to hydrogen bonding between neighboring serine and histidine amino acids located on the arms of neighboring monomers. At low pH, the histidine side chains are protonated and hydrogen bonding does not occur, creating weakly elastic hydrogels. At pH 7.4, above the pKa of the histidine imidazole group, cooperative hydrogen bonding occurs, stabilizing the self-assembled worm-like micelles and creating a strong viscoelastic hydrogel.[35] This unique architecture of C_{16}GSH makes it possible to create hydrogels spanning a wide range of stiffness. Additionally, C_{16}GSH hydrogels were shown to be capable of supporting NIH/3T3 fibroblast growth *in vitro*.[35]

In this work, the C_{16}GSH hydrogel was optimized through a series of *in vitro* and *in vivo* tests to serve as a filler gel material to be used in conjunction with a nerve guide conduit for peripheral nerve regeneration. A commercially available collagen gel was used as a benchmark as collagen gels have been shown to be beneficial both *in vitro* and *in vivo* for PNI.[36,37] First, a series of *in vitro* tests designed to mimic *in vivo* conditions was used to evaluate the hydrogel's ability to promote spreading, proliferation, and migration of Schwann cells. Following *in vitro* optimization, an *in vivo* subcutaneous implantation model was used to investigate the biocompatibility and degradation rate of the hydrogels. Used together, this set of *in vitro* and *in vivo* tests provides a useful methodology to screen and optimize hydrogels for peripheral nerve regeneration applications. The work reported here represents a critical step in developing a hydrogel for peripheral nerve regeneration before the use of a small animal injury model. Ultimately, the creation and use of an improved filler gel material in conjunction with hollow synthetic nerve guides will allow clinicians to repair long gap peripheral nerve injuries without the undesirable side effects of the current state of the art treatment, autografting.

Materials and Methods

PA synthesis

The GSH peptide was purchased fully protected on rink amide resin (China Tech Peptides Co., Suzhou, China) or synthesized on rink amide resin (Anaspec, Fremont, CA) using an automated PS3 Benchtop Peptide Synthesizer (Protein Technologies, Tucson, AZ). Fatty acid tails were conjugated to the lysine residue of the peptide as described previously[35] to create C_{16}GSH PAs (Fig. 1). The synthesis products were precipitated in diethyl ether and purified to above 90% purity on a Shimadzu CBM-20A high-performance liquid chromatography (HPLC) system in reverse phase, employing a Waters Symmetry 300 semipreparative C8 column. Product identity was confirmed by mass spectrometry, employing an Applied Biosystems 4700 Proteomics Analyzer, and purity was determined using analytical HPLC with a Waters Symmetry 300 analytical column. Exact concentrations were determined by UV spectroscopy,[38] and it was determined that the peptides accounted for 60% of the measured mass of peptide salts. This correction was taken into account when considering molarity.

Hydrogel preparation

C_{16}GSH stock solutions were prepared at 2 wt% in MilliQ water at pH 4 and sterilized by filtration through a 0.8/0.2 μm Supor® Membrane filter (Pall Life Sciences, Port Washington, NY). PA solutions were heated to 50°C and sonicated for 5 min to ensure complete dissolution. PA solutions were then cooled to room temperature and further diluted with MilliQ water to specified concentrations before use. For *in vivo* studies, C_{16}GSH stock solutions were diluted to 2 and 0.2 wt% in water, raised to pH 6.5 using 1 M NaOH (Sigma Aldrich, Milwaukee, WI), and loaded into 1-mL sterile syringes. A buffer solution of 2× phosphate-buffered saline

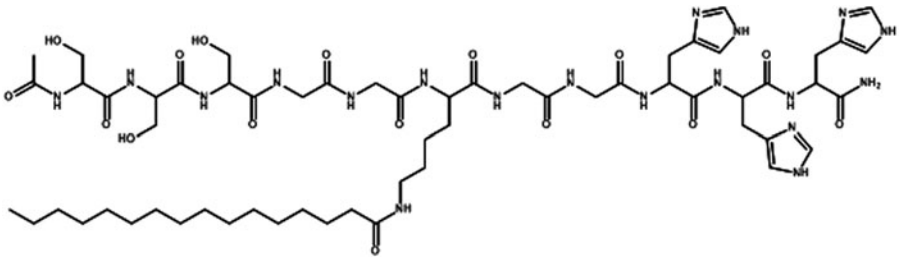

FIG. 1. Chemical structure of the peptide amphiphile (PA), C_{16}GSH.

(PBS) was added and mixed thoroughly to achieve a concentration of 1 and 0.1 wt%, respectively, and a pH of 7.4.

Type I bovine collagen (Sigma Aldrich) was used as received (0.3 wt%). The manufacturer's instructions were followed for the gelling procedure. Briefly, the acidic collagen solution was mixed 8:1 with 10× PBS, and the pH was adjusted to 7.4 using 1 μL drops of 0.1 M NaOH. Collagen solutions were kept on ice before use to prevent gelation. Collagen solutions were gelled by incubation at 37°C for 1 h.

Rheology

Oscillatory shear rheology was performed on an Anton Paar Physica MCR 301 using a 25-mm top plate. The measurement distance was set to 1 mm and the samples were measured in a humidity chamber set at 20°C. Collagen samples were prepared in MilliQ water and 10×PBS as previously described (Sigma Aldrich) and kept on ice until use. Collagen solutions were equilibrated for 1 h at 37°C in the humidity chamber. Frequency sweeps were performed between 1 and 10 Hz using a fixed 1% strain. Two sweeps were performed for each sample, and the data from the second sweep are reported.

Cell culture

Cell culture reagents were purchased from Gibco (Life Technologies, Carlsbad, CA) unless otherwise noted. Rat Schwannoma cells, RT4-D6P2T (ATCC, Manassas, VA), were cultured in Dulbecco's modified Eagle's medium (DMEM) supplemented with 10% fetal bovine serum and 1% penicillin–streptomycin (P-S). Cells were incubated at 37°C in an atmosphere of 5% CO_2. Cell experiments were performed using passage 5–10 cells.

Scanning electron microscopy

C_{16}GSH solutions were cast onto glass coverslips (10 μL per coverslip) and allowed to equilibrate for 20 min. Gel cross-linking was achieved by adding 1 μL of 0.1 M NaOH and waiting for 30 min. Coverslips were placed at the bottom of an eight-well chamber slide (Nunc; Thermo Scientific, Waltham, MA) and washed thrice with PBS and thrice with serum-free DMEM. Schwann cells were trypsinized, suspended in complete medium, and added at a density of 5000 cells per well. Cells were allowed to attach and spread for a period of 24 h. Samples were then washed with PBS and fixed with 4% formaldehyde for 15 min. Samples were fixed a second time with 2% glutaraldehyde in 0.1 M sodium cacodylate buffer, washed thrice with 0.1 M sodium cacodylate buffer, and postfixed in 1% osmium tetroxide in 0.1 M sodium cacodylate buffer for 1 h. Samples were again washed thrice with 0.1 M sodium cacodylate to remove excess osmium tetroxide and exposed to a gradient of increasing ethanol in water until 100% ethanol was reached. Samples were then subjected to critical point drying on a Tousimis AutoSamdri-815, Series A. Dried samples were sputter coated with platinum using a Tousimis sputter coater. Scanning electron microscopy (SEM) was performed on a Hitachi S-5000 high-resolution, cold-field emission SEM.

Cell proliferation

C_{16}GSH solutions were cast into Corning half-area 96-well plates (Sigma Aldrich) at a volume of 30 μL per well, resulting in a solution of ~1 mm in height. The solution was allowed to rest for 20 min before gel cross-linking was initiated by the addition of 1 μL of 50% NaOH. Gels were then washed 10 times with PBS. Gels were sterilized with 5×P-S in PBS for 1 h. Gels were washed with DMEM (without serum) five times and incubated at 37°C for 1 h. Schwann cells were added to wells at a density of 2500 cells per well in complete medium. After 24 h of growth, cells were imaged on a Nikon Eclipse TE200 microscope. After 48 h, PrestoBlue® (Invitrogen, Carlsbad, CA) was added to the wells to achieve a final concentration of 10% by volume. After 3 h of incubation, 100 μL of reaction solution was transferred to a fresh well plate, and absorbance was read on a Tecan plate reader (570 nm). Transfer of solutions before assay readout was necessary due to interference in the absorbance signal with the presence of hydrogel.

Migration

C_{16}GSH solution was loaded into the inlet ports of Iuvo™ Microchannel 5250 plates (Thermo Scientific), 1 mm wide×5.25 mm long×140 μm high. The solution was allowed to rest for 20 min before gel cross-linking was initiated by adding 1 μL of 0.1 M NaOH to the outlet port. After 1 h, gels inside the channels were washed five times with PBS by adding 3 μL to the inlet port allowing 5 min for passive pumping to occur. Gels inside the channels were sterilized with 5× P-S in PBS for 1 h, washed with DMEM (without serum) five times, and incubated at 37°C for 1 h. Schwann cells were added at a density of 2000 cells per channel to the outlet port in complete medium. Each microchannel was then checked visually to ensure cells were only present in the outlet port area. Cells were allowed to migrate across gel-filled channels for 6 days and media were replenished on days 2 and 5. On day 6, media were removed, and cells were fixed and stained with Hoechst 33242 (Sigma) and FITC-Phalloidin (Invitrogen). Images of migration were taken on a Zeiss LSM 700 laser scanning confocal microscope. ImageJ software was used to count cell nuclei that had migrated into the channel from the outlet port.

Subcutaneous biocompatibility

Female BALB/c mice (Charles River Laboratories, Sulzfeld, Germany) were housed, five animals per cage, kept with water *ad libitum*, exposed to an artificial light–dark regime, and fed with regular chow. To assess the biocompatibility of the C_{16}GSH hydrogels, 38 BALB/c mice were given subcutaneous implantations of one of the four following materials: 0.1 wt% C_{16}GSH hydrogel ($n=10$), 1 wt% C_{16}GSH hydrogel ($n=10$), collagen gel ($n=9$), or a sham-operated PBS control ($n=9$). The C_{16}GSH hydrogels were prepared as previously described in 1-mL syringes and stored at 37°C overnight. Collagen gel was prepared as described earlier, with solution being preloaded into 1-mL syringes and heated to 37°C overnight to induce gelation.

Mice were anesthetized using isoflurane (1.5–3% in O_2), their interscapular region shaved, and a small incision (~2 cm) made on the right dorsal side. A sterile 1-mL syringe was used to inject 100 μL under the skin without a needle. The incision was then closed with two 4.0 silk sutures (Ethicon, Somerville, NJ). All animal procedures followed NIH guidelines for the care and use of laboratory animals and were

approved by the University of Chicago's Institutional Animal Care and Use Committee (Protocol No. 72297, Chicago, IL).

Histology and immunohistochemistry

Mice were euthanized at time points of 3, 10, and 30 days postimplantation to study early (days 3 and 10) and late (day 30) *in vivo* response. Following euthanization, the implantation bed and surrounding tissues were explanted, and blood samples were collected from the thoracic cavity. The explants were fixed in 10% neutral buffered formalin for 8 h, dehydrated in a graded series of ethanol, transferred to xylene, and embedded in paraffin. The samples were then sectioned into 5–7-μm-thick slices, deparaffinized, and rehydrated. Sections were stained with hematoxylin and eosin (H&E) or processed for immunohistochemistry.

To assess host immune response and vascularization, rat anti-mouse CD45 antibody (1:10, 550539; BD, Franklin Lakes, NJ), rat anti-mouse F4/80 antibody (1:200, MCA497GA; AbD Serotec, Oxford, United Kingdom), and goat polyclonal anti-mouse CD31 antibody (1:200, sc-1506; Santa Cruz Biotechnology, Santa Cruz, CA) were used to detect leukocytes, macrophages, and endothelial cells, respectively. Tissue sections were deparaffinized in xylene and rehydrated through serial dilutions of ethanol. Sections were then incubated in antigen retrieval buffer (S1699; DAKO, Glostrup, Denmark) and heated at 97°C for 20 min in a steamer. Primary antibodies were applied to the sections and incubated in a humidified chamber at room temperature for 1 h. Slides were washed with PBS and incubated for 30 min at room temperature with the secondary antibodies. Secondary antibodies included rat adsorbed biotinylated horse anti-mouse IgG antibody (1:100, BA-2001; Vector Laboratories, Burlingame, CA), biotinylated rabbit anti-rat IgG antibody (10 μg/mL, BA-4001; Vector Laboratories), and biotinylated horse anti-goat IgG antibody (1:200, BA-9500; Vector Laboratories). Finally, antigen–antibody binding was detected by the Elite kit (PK-6100; Vector Laboratories) and the DAB (K3468; DAKO) system. All sections were evaluated using bright-field microscopy (Leica DMI6000 B, Wetzlar, Germany).

Enzyme-linked immunosorbent assay

Blood samples were collected and the serum was separated out by centrifugation. Serum was kept at −80°C until time of use. Circulating IgG was assayed using an enzyme-linked immunosorbent assay (ELISA) kit (Bethyl Laboratories, Montgomery, TX). Briefly, microtiter plates were coated with goat anti-mouse IgG-Fc for 1 h at room temperature. Plates were washed with 50 mM Tris, 0.14 M NaCl, and 0.05% Tween 20, and then blocked with 50 mM Tris, 0.14 M NaCl, and 1% bovine serum albumin (BSA) for 30 min. Samples and reference serum were serially diluted in 50 mM Tris, 0.14 M NaCl, 1% BSA, and 0.05% Tween 20. Following 1 h of incubation and washing steps, an HRP-conjugated anti-IgM or anti-IgG detection antibody was added. After addition of substrate solution, the reaction was stopped with 0.18 M H_2SO_4. The absorbance was measured at 450 nm on a Tecan plate reader. A four-parameter fitting equation was used according to the manufacturer's instructions to convert absorbance to concentration using reference serum as a standard.

Statistical analysis

Experimental values are expressed as mean ± standard deviation. Statistical significance was calculated using a one-way ANOVA with Tukey's or Dunnett's *post hoc* correction with $p < 0.05$ or $p < 0.01$, as indicated.

Results

Tunable mechanical properties

Physical properties of the C_{16}GSH hydrogel system are compared with properties of a commercially available collagen gel (Table 1). At physiological pH, increasing the concentration of C_{16}GSH directly correlates to an increase in the storage modulus of the material spanning a range from 0.3 kPa at a concentration of 0.05 wt% up to 9.7 kPa at the highest concentration tested, 1 wt%.[35] Collagen, prepared according to the manufacturer's instructions, has a storage modulus of 1 kPa and a concentration of 0.3 wt%. Thus, at a bulk concentration of 0.3 wt%, C_{16}GSH is approximately six times stiffer than the collagen gel. Conversely, at a stiffness of 1 kPa, collagen (0.3 wt%) is a denser gel than C_{16}GSH at equivalent stiffness (0.1 wt%).

Schwann cell spreading

To investigate how cells interact with the materials, Schwann cells were grown on C_{16}GSH hydrogels and the control surface, collagen, for 18 h and imaged using bright-field microscopy. For this work, rat Schwannoma cells, which have been shown in previous work to be similar to primary Schwann cells, were used.[39] As stiffness was increased, less spreading was observed (Fig. 2A–C). Cells spread most on the softest gel (0.1 wt%, $G' = 0.92$ kPa) (Fig. 2D). There was also minimal spreading on the collagen gel (Fig. 2E).

Cells were also grown on gels for 24 h and processed for SEM. From these images, it is possible to visualize the gel fibers. Cells grown on 0.1 wt% C_{16}GSH gels were able to attach, spread, and migrate as evident by the appearance of broken fibers near the trailing edge of the cells (Fig. 3A). On collagen, cells were able to attach, but exhibited less spreading than was seen with the 0.1 wt% C_{16}GSH gel (Fig. 3B). C_{16}GSH and collagen at these concentrations have roughly equivalent stiffness, 0.92 and 1.07 kPa, respectively (Table 1).

Schwann cell in vitro *viability*

Proliferation assays were utilized as a measure of cell biocompatibility. Schwann cells were grown on gel surfaces

Table 1. Comparison of Stiffness for C_{16}GSH and Collagen Hydrogels of Varying Concentrations

Material	*Weight%*	*Storage modulus, G′ (Pa)*	*Young's modulus, E (Pa)*
C_{16}GSH	1	9.66×10^3	2.90×10^4
	0.5	7.19×10^3	2.16×10^4
	0.2	4.16×10^3	1.25×10^4
	0.1	9.16×10^2	2.75×10^3
	0.05	3.37×10^2	1.01×10^3
Collagen	~0.3	1.07×10^3	3.21×10^3

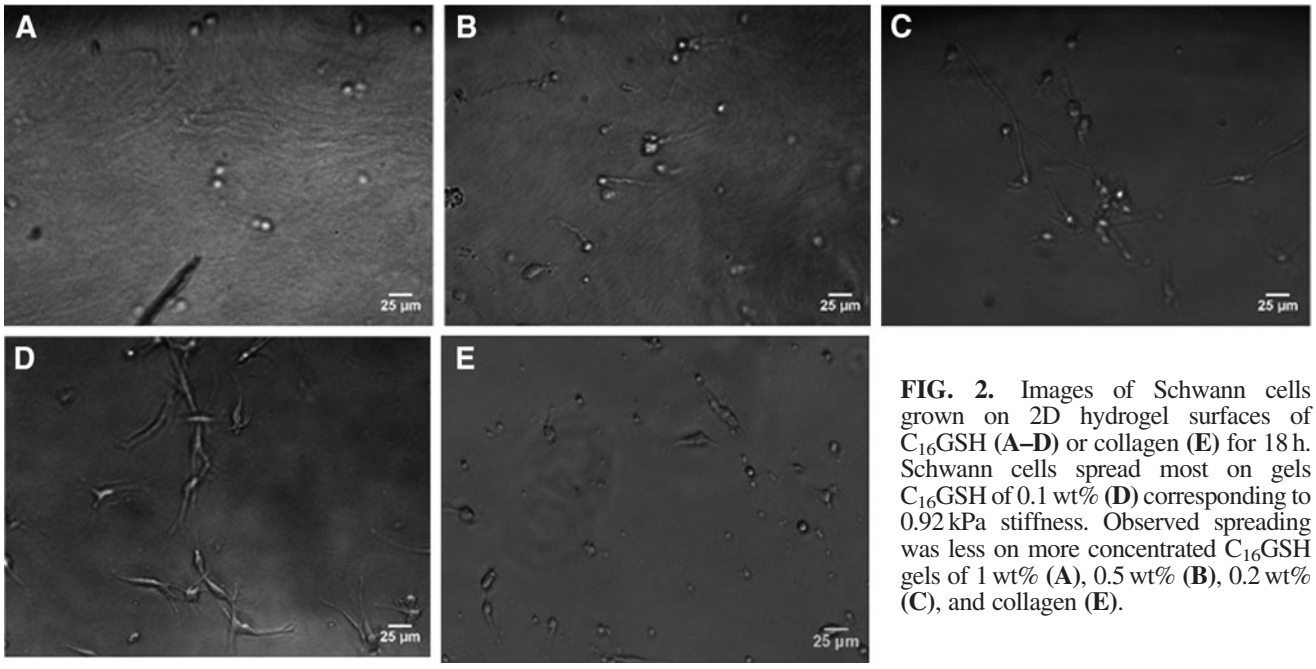

FIG. 2. Images of Schwann cells grown on 2D hydrogel surfaces of C_{16}GSH **(A–D)** or collagen **(E)** for 18 h. Schwann cells spread most on gels C_{16}GSH of 0.1 wt% **(D)** corresponding to 0.92 kPa stiffness. Observed spreading was less on more concentrated C_{16}GSH gels of 1 wt% **(A)**, 0.5 wt% **(B)**, 0.2 wt% **(C)**, and collagen **(E)**.

for 2 days, after which proliferation was quantified. Viable cell number on all concentrations of C_{16}GSH gel was higher than that of proliferation on collagen gel, a result that was found to be statistically significant (ANOVA, Dunnett's Test, $p < 0.01$) (Fig. 4). No statistical difference was found between C_{16}GSH concentrations.

3D Schwann cell migration

To better mimic the cellular environment during peripheral nerve repair, a microchannel experiment was used to measure Schwann cell migration (Fig. 5). Cells were seeded at the open inlet of closed channels, 1 mm wide, 140 μm high, and 5.25 mm long, filled with hydrogel. Cells were allowed to grow and migrate through the microchannel in response to crowding at the inlet and availability of nutrients (no additional growth factors were added). After a period of 6 days, roughly equivalent to the cellular migration phase *in vivo*,[12] representative images show a longitudinal slice of the microchannel where cells have migrated from the inlet port (white arc) along the channel through a C_{16}GSH or a collagen hydrogel (Fig. 5). When the channel was filled with a collagen gel (Fig. 5A), only a few cells migrated into the channel. Comparatively, when C_{16}GSH was used at 0.2 wt% (Fig. 5B), a large increase in migrated cells was seen. Additionally, cells exhibit a spindle-like morphology and alignment along the direction of the channel. Using a 0.05 wt% C_{16}GSH increases cell migration into the hydrogel-filled channel (Fig. 5C).

Total number of migrated cells for each condition was analyzed using ImageJ software to count the number of stained cell nuclei that had migrated into the channel from the outlet port (Fig. 6). For channels filled with collagen or 0.5 wt% C_{16}GSH, only a few cells were able to migrate into the channel, likely due to the high density of fibers present, seen previously in SEM.[35] At 0.2 wt% C_{16}GSH, a critical

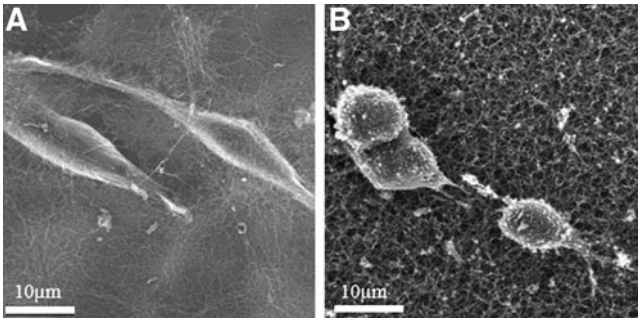

FIG. 3. Scanning electron micrographs of Schwann cells grown on 2D surfaces of 0.1 wt% C_{16}GSH **(A)** and collagen **(B)** gels after 24 h. Conditions of 0.1 wt% C_{16}GSH and collagen have roughly equivalent stiffness, 0.92 and 1.07 kPa, respectively.

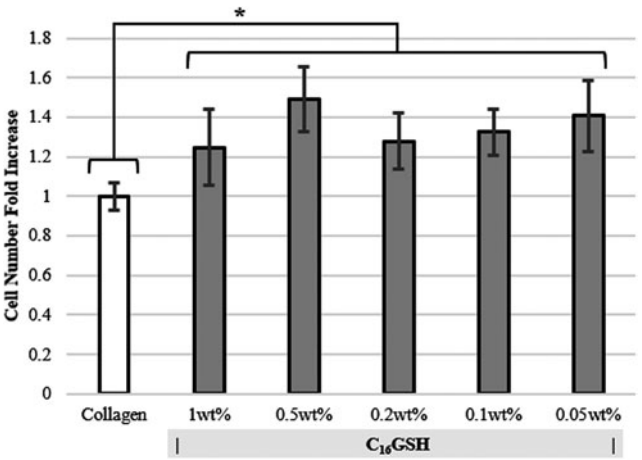

FIG. 4. Proliferation of Schwann cells on collagen and C_{16}GSH gels after 48 h (mean ± SD, $*p < 0.01$, ANOVA, Dunnett's test). At all concentrations, cells proliferate more on C_{16}GSH gels than on collagen.

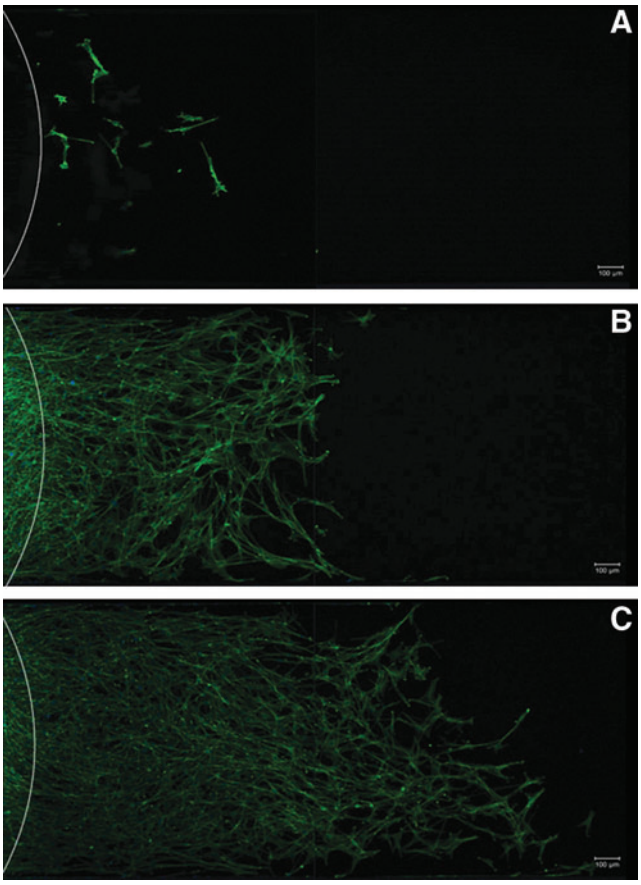

FIG. 5. Representative images of Schwann cells migrating through microchannels filled with collagen **(A)** and 0.2 wt% **(B)** or 0.05 wt% **(C)** C_{16}GSH hydrogels. Cells have migrated from the inlet area (*white arc*) on the left toward the right over a period of 6 days without additional growth factors.

porosity or mechanical property was achieved, where below this concentration Schwann cell migration was permitted. The greatest number of migrating cells occurred at 0.05 wt% C_{16}GSH.

In vivo *biocompatibility*

To assess the biocompatibility and degradation of the C_{16}GSH hydrogels *in vivo*, a murine subcutaneous implantation model was used. Gels were inserted into the subcutaneous space on the dorsal scapular region. No evidence of irritation, redness, or swelling was observed at the site of subcutaneous implantation for any of the test groups over the course of the study. The gels were implanted in the subcutaneous space and not restrained, thus movement and relocation of the gel were expected. During histological analysis, clear evidence of the 1 wt% C_{16}GSH gel was seen at days 3 and 10 and with a smaller area at day 30 (Fig. 7). The softer 0.1 wt% C_{16}GSH and collagen gels were not clearly visible in histology slides. This result was expected considering the soft nature of the 0.1 wt% C_{16}GSH and collagen gels and the freedom of movement possible for the unconfined gel in the subcutaneous space. However, in future studies regarding peripheral nerve regeneration, the gel would be confined within a solid conduit and enclosed between severed nerve ends and therefore not be able to dissipate within the body.

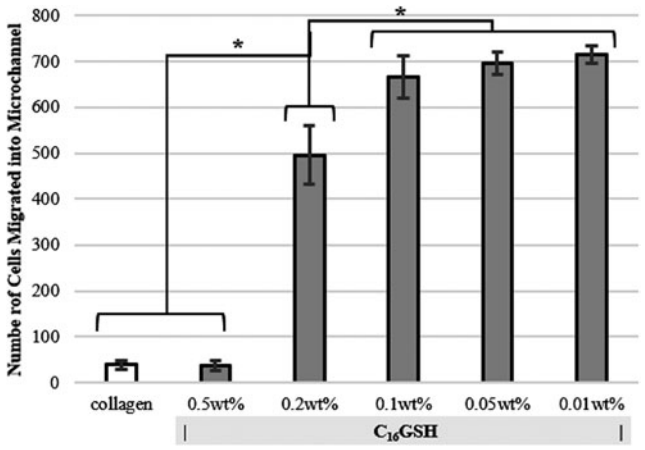

FIG. 6. Migration of Schwann cells through three-dimensional (3D) michrochannels of collagen or C_{16}GSH gels. Calculated number of cells entering the microchannel from the entrance port for each gel, as calculated using ImageJ software. (mean ± SD, $*p < 0.01$, ANOVA, Dunnett's test).

At day 3, a large area of 1 wt% C_{16}GSH was seen with infiltrating cells, fibroblasts and macrophages (Fig. 7). The presence of macrophages at the edge of the implanted gel was confirmed by positive (brown) staining against F4/80. At this time point, there was no visible fibrous capsule formation at the gel interface and no evidence of multinucleated giant cells.

At day 10, cells migrated into roughly 30% into the gel and started to degrade the material (Fig. 7). At this time point, there was also positive F4/80 staining, indicating the presence of macrophages. Interestingly, at day 10, robust blood vessel formation can be seen inside the gel area, indicating that the gel was able to support angiogenesis. Functional blood vessel formation is confirmed by the presence of red blood cells within the lumen of the blood vessel (black arrows, Fig. 8).

By day 30, the gel was mostly degraded and only a small thin section of gel was visible. At this late time point, the 1 wt% C_{16}GSH gel was almost completely integrated into the surrounding tissue, and the presence of macrophages was greatly reduced as indicated by a lack of F4/80 staining.

Immune response

To investigate if subcutaneous implantation caused any adverse systemic effects, an ELISA was used to measure the levels of circulating total IgG in the blood at each time point. At each time point, no statistical difference was measured between treatment groups.

Discussion

To achieve the same efficacy as nerve autografting, the current standard of care, nerve guide conduits need to be improved beyond their current hollow tube design. Several strategies have been put forward, including intraluminal channels, cellular supplementation, and hydrogels.[40] Several natural hydrogel materials have been studied to fill this need,

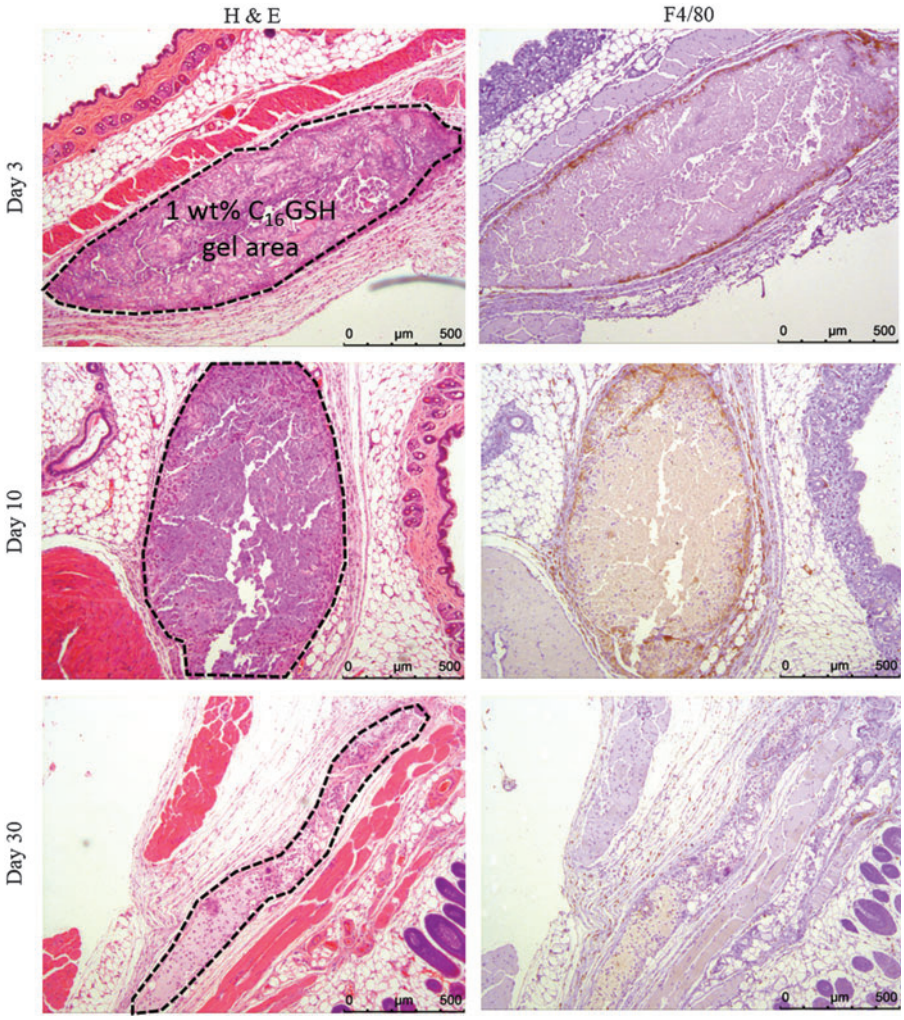

FIG. 7. Histological images of 1 wt% C_{16}GSH hydrogels implanted subcutaneously at days 3, 10, and 30. *Dashed outlines* indicate the gel implant area. Over a 30-day period, gels are infiltrated by cells and degrade (hematoxylin and eosin [H&E] staining). The presence of macrophages is confirmed with F4/80 staining at days 3 and 10 and is significantly reduced by day 30.

including collagen, laminin, and hyaluronic acid.[10] Collagen hydrogels, in particular, have shown some efficacy both *in vitro* and *in vivo* for peripheral nerve regeneration and thus provide a useful benchmark for this work.[13–15] In this study, we develop a synthetic hydrogel based on the self-assembly of PAs for the application of nerve guide conduit filler.

C_{16}GSH, a PA developed previously, was shown to have ideal mechanical properties for soft tissue engineering.[35] At physiological pH, amino acids in the head group of the PA participate in cooperative hydrogen bonding, which effectively cross-links the worm-like micelle assembly. By increasing the concentration, a span of moduli can be achieved ranging from a storage modulus of 0.3–10 kPa (Table 1). This large range in stiffness is possible because the PA hydrogels scale with concentration by increasing the fiber density and entanglements. For comparison, collagen, as supplied (0.3 wt%), had a modulus of 1 kPa. With collagen, scaling the concentration of the material to scale the modulus is limited due to the nature of collagen self-assembly as fibers gel by associating in a triple helix.[41]

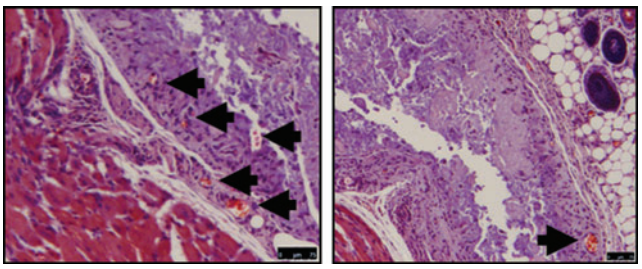

FIG. 8. Day 10 histological images of 1 wt% C_{16}GSH implanted gels showing spontaneous development of blood vessels within the gel (*black arrows*). Scale bar is 75 µm.

Schwann cells, considered the first responders of peripheral nerve repair, must spread, proliferate, and migrate into the injury space to guide neurons and achieve functional repair. Thus, a hydrogel designed for peripheral nerve repair applications must enhance the activity of this cell population. In this study, we show that Schwann cells spread and elongated best on the lowest concentration of C_{16}GSH gels tested (0.1 wt%) (Fig. 2). On gels of equivalent stiffness, Schwann cells spread more on C_{16}GSH than on collagen (Fig. 3). The importance of fiber density is highlighted since at these concentrations, C_{16}GSH and collagen have equivalent stiffnesses; however, spreading was greatly improved on the C_{16}GSH surface, which has a lower fiber density. Additionally, the Schwann cells display a polarized spindle morphology, which is consistent with a migratory phenotype.[42]

As a measure of cell viability, proliferation of cells grown on the surfaces of gels was measured after 2 days. Schwann cells proliferated more on C_{16}GSH, at all concentrations, compared with collagen gels (Fig. 4). Interestingly, there is no statistical difference or trend between the varying concentrations of C_{16}GSH gels. This result suggests that although cell proliferation is a commonly used *in vitro* test, it may not be sufficient in analyzing subtle differences in cell preference based on substrate stiffness.

With the eventual goal of peripheral nerve regeneration inside a hollow conduit filled with gel, a 3D microchannel migration assay was used to best mimic conditions that the cells face *in vivo*. Using a 3D microchannel assay, large differences in cell migration were evident between gel concentrations that were not evident in the simple 2D proliferation assay. For collagen and 0.5 wt% C_{16}GSH, very few cells were able to migrate, likely due to the increased density of the gels. At 0.2 wt% C_{16}GSH, the density and stiffness of the gel is permissive to migration, and a large increase in the number of cells migrated into the microchannel was seen. Migration was maximized at a C_{16}GSH concentration of 0.01 wt% (Fig. 6). The rate of cell migration and gel wt% preference *in vivo* may change with the addition of other cell types and digesting enzymes. The trend, however, is informative for the design of hydrogels for this application. This result also highlights the importance of using a 3D assay to replicate an environment where 3D interaction is important. Using the 2D assays provides some information, mainly that cells spread better on gels of relevant stiffness, but have similar viability. The 3D migration assay was able to capture what is also likely a key component to the cell–material interaction for this application: fiber density. Further work is needed to decouple the effect of stiffness and fiber density as the two are inherently linked in the C_{16}GSH system.

Last, C_{16}GSH gels were implanted subcutaneously and shown to degrade and support regeneration without causing inflammation or a foreign body immune response. Cells migrated well into the tissue, including macrophages, which play an important role in tissue regeneration.[43] At the border between native tissue and the PA gel implant, there was no evidence of a fibrous capsule or chronic inflammation in the form of multinucleated giant cells (Fig. 7).[44] After 10 days of implantation, new blood vessel formation was evident inside the gel implant (Fig. 8). This result is important as previous PA-based gels required the use of growth factors to promote angiogenesis.[45] Robust blood vessel formation is a key process in peripheral nerve regeneration, and the presence of new blood vessels has been shown to improve nerve regeneration *in vivo*.[46] By 30 days, the gel has mostly been degraded or integrated into the surrounding tissue. In sum, PA gels are able to support cell ingrowth, blood vessel formation, and degradation. Although the environment within the nerve guide conduit will be different, the *in vivo* biocompatibility done here represents an important first step in studying immune response and regenerative potential of a biomaterial.

Finally, systemic immune response was analyzed by measuring circulating IgG levels at each time point. Elevated levels of IgG would indicate an adaptive immune response by the body to foreign materials.[47] However, we found no statistical difference between the sham-operated PBS group and the C_{16}GSH and collagen gel implant groups (Fig. 9). This result indicates that implantation of both the C_{16}GSH and collagen gels did not cause a systemic immune response.

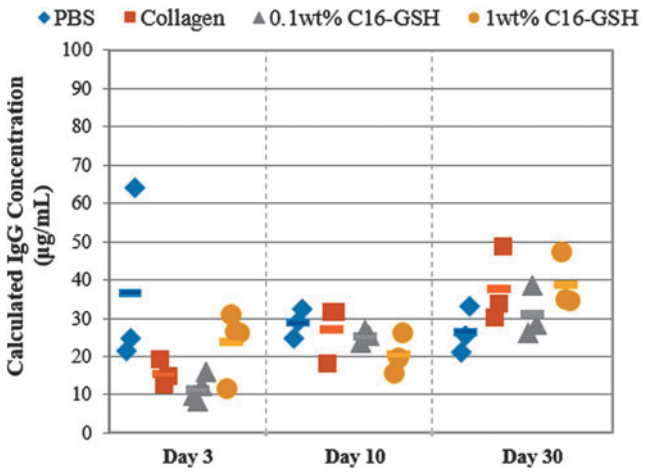

FIG. 9. Systemic antibody production as measured by total IgG ELISA. No statistical difference was measured between treatment groups within each time point (ANOVA with Tukey's *post hoc* correction).

With this set of *in vitro* and *in vivo* assays, a PA hydrogel, C_{16}GSH, was studied and compared with a benchmark of collagen gel for the application of a luminal filler for conduit-mediated peripheral nerve repair. In each *in vitro* assay, designed to replicate *in vivo* conditions, the C_{16}GSH gel surpassed the collagen gel control in enhancing the activity of Schwann cells. When implanted *in vivo*, C_{16}GSH did not cause any local or systemic immune response. Future work will continue to develop the C_{16}GSH hydrogels as a conduit filler using a small animal PNI model.

Acknowledgments

This work was supported by the Armed Forces Institute for Regenerative Medicine (AFIRM) and the American Heart Association Postdoctoral Fellowship granted to E.J.C. Histological sample preparation and staining were completed by the University of Chicago's Human Tissue Resource Center (HTRC, Biological Science Division).

Disclosure Statement

The authors acknowledge that no competing financial interests exist.

References

1. Noble, J., Munro, C., and Prasad, V. Analysis of upper and lower extremity peripheral nerve injuries in a population of patients with multiple injuries. J Trauma **45,** 116, 1998.
2. Ray, W.Z., and Mackinnon, S.E. Management of nerve gaps: autografts, allografts, nerve transfers, and end-to-side neurorrhaphy. Exp Neurol **223,** 77, 2010.
3. Mackinnon, S. New directions in peripheral nerve surgery. Ann Plast Surg **22,** 257, 1989.
4. Seckel, B. Enhancement of peripheral nerve regeneration. Muscle Nerve **13,** 785, 1990.

5. Meek, M.F., and Coert, J.H. US Food and Drug Administration/Conformit Europe-approved absorbable nerve conduits for clinical repair of peripheral and cranial nerves. Ann Plast Surg **60,** 110, 2008.
6. Kehoe, S., Zhang, X.F., and Boyd, D. FDA approved guidance conduits and wraps for peripheral nerve injury: a review of materials and efficacy. Injury **43,** 553, 2012.
7. Bell, J., and Haycock, J. Next generation nerve guides: materials, fabrication, growth factors, and cell delivery. Tissue Eng Part B Rev **18,** 116, 2011.
8. Angius, D., *et al.* A systematic review of animal models used to study nerve regeneration in tissue-engineered scaffolds. Biomaterials **33,** 8034, 2012.
9. Chalfoun, C.T., Wirth, G.A. and Evans, G.R.D. Tissue engineered nerve constructs: where do we stand? J Cell Mol Med **10,** 309, 2006.
10. Lin, Y.-C., and Marra, K.G. Injectable systems and implantable conduits for peripheral nerve repair. Biomed Mater **7,** 024102, 2012.
11. Biazar, E., *et al.* Types of neural guides and using nanotechnology for peripheral nerve reconstruction. Int J Nanomedicine **5,** 839, 2010.
12. Belkas, J.S., Shoichet, M.S., and Midha, R. Peripheral nerve regeneration through guidance tubes. Neurol Res **26,** 151, 2004.
13. Satou, T., *et al.* A morphological study on the effects of collagen gel matrix on regeneration of severed rat sciatic nerve in silicone tubes. Pathol Int **36,** 199, 1986.
14. Madison, R., da Silva, C.F., Dikkes, P., Chiu, T.H., and Sidman, R.L. Increased rate of peripheral nerve regeneration using bioresorbable nerve guides and a laminin-containing gel. Exp Neurol **88,** 767, 1985.
15. Chamberlain, L.J., Yannas, I. V, Hsu, H.P., Strichartz, G.R., and Spector, M. Near-terminus axonal structure and function following rat sciatic nerve regeneration through a collagen-GAG matrix in a ten-millimeter gap. J Neurosci Res **60,** 666, 2000.
16. Charriere, G., Bejot, M., Schnitzler, L., Ville, G., and Hartmann, D.J. Reactions to a bovine collagen implant. J Am Acad Dermatol **21,** 1203, 1989.
17. Tan, A., Rajadas, J., and Seifalian, A.M. Biochemical engineering nerve conduits using peptide amphiphiles. J Control Release **163,** 342, 2012.
18. Trent, A., Marullo, R., Lin, B., Black, M., and Tirrell, M. Structural properties of soluble peptide amphiphile micelles. Soft Matter **7,** 9572, 2011.
19. Greenfield, M.A., Hoffman, J.R., de la Cruz, M.O., and Stupp, S.I. Tunable mechanics of peptide nanofiber gels. Langmuir **26,** 3641, 2010.
20. Morisco, A., *et al.* Micelles derivatized with octreotide as potential target-selective contrast agents in MRI. J Pept Sci **15,** 242, 2009.
21. Bull, S.R., Guler, M.O., Bras, R.E., Meade, T.J., and Stupp, S.I. Self-assembled peptide amphiphile nanofibers conjugated to MRI contrast agents. Nano Lett **5,** 1, 2005.
22. Hartgerink, J.D., Beniash, E., and Stupp, S.I. Self-assembly and mineralization of peptide-amphiphile nanofibers. Science **294,** 1684, 2001.
23. Spoerke, E.D., Anthony, S.G., and Stupp, S.I. Enzyme directed templating of artificial bone mineral. Adv Mater **21,** 425, 2009.
24. Branco, M.C., and Schneider, J.P. Self-assembling materials for therapeutic delivery. Acta Biomater **5,** 817, 2009.
25. Webber, M.J., Matson, J.B., Tamboli, V.K., and Stupp, S.I. Controlled release of dexamethasone from peptide nanofiber gels to modulate inflammatory response. Biomaterials **33,** 6823, 2012.
26. Bitton, R., *et al.* Self-assembly of model DNA-binding peptide amphiphiles. Langmuir **21,** 11888, 2005.
27. Tu, R.S., *et al.* Cooperative DNA binding and assembly by a bZip peptide-amphiphile. Soft Matter **6,** 1035, 2010.
28. Black, M., *et al.* Self-assembled peptide amphiphile micelles containing a cytotoxic T-cell epitope promote a protective immune response in vivo. Adv Mater **24,** 3845, 2012.
29. Standley, S.M., *et al.* Induction of cancer cell death by self-assembling nanostructures incorporating a cytotoxic peptide. Cancer Res **70,** 3020, 2010.
30. Garg, A., Tisdale, A.W., Haidari, E., and Kokkoli, E. Targeting colon cancer cells using PEGylated liposomes modified with a fibronectin-mimetic peptide. Int J Pharm **366,** 201, 2009.
31. Webber, M.J., Berns, E.J., and Stupp, S.I. Supramolecular nanofibers of peptide amphiphiles for medicine. Isr J Chem **53,** 1, 2013.
32. Tysseling, V.M., *et al.* Self-assembling peptide amphiphile promotes plasticity of serotonergic fibers following spinal cord injury. J Neurosci Res **88,** 3161, 2010.
33. Tysseling-Mattiace, V.M., *et al.* Self-assembling nanofibers inhibit glial scar formation and promote axon elongation after spinal cord injury. J Neurosci **28,** 3814, 2008.
34. Bond, C.W., *et al.* Peptide amphiphile nanofiber delivery of sonic hedgehog protein to reduce smooth muscle apoptosis in the penis after cavernous nerve resection. J Sex Med **8,** 78, 2011.
35. Lin, B.F., *et al.* pH-responsive branched peptide amphiphile hydrogel designed for applications in regenerative medicine with potential as injectable tissue scaffolds. J Mater Chem **22,** 19447, 2012.
36. Dubey, N., Letourneau, P.C., and Tranquillo, R.T. Guided neurite elongation and schwann cell invasion into magnetically aligned collagen in simulated peripheral nerve regeneration. Exp Neurol **158,** 338, 1999.
37. Ceballos, D., *et al.* Magnetically aligned collagen gel filling a collagen nerve guide improves peripheral nerve regeneration. Exp Neurol **158,** 290, 1999.
38. Kuipers, B.J.H., and Gruppen, H. Prediction of molar extinction coefficients of proteins and peptides using UV absorption of the constituent amino acids at 214 nm to enable quantitative reverse phase high-performance liquid chromatography-mass spectrometry analysis. J Agric Food Chem **55,** 5445, 2007.
39. Hai, M., Muja, N., DeVries, G.H., Quarles, R.H., and Patel, P.I. Comparative analysis of Schwann cell lines as model systems for myelin gene transcription studies. J Neurosci Res **69,** 497, 2002.
40. Huang, Y.-C., and Huang, Y.-Y. Biomaterials and strategies for nerve regeneration. Artif Organs **30,** 514, 2006.
41. Piechocka, I.K., van Oosten, A.S.G., Breuls, R.G.M., and Koenderink, G.H. Rheology of heterotypic collagen networks. Biomacromolecules **12,** 2797, 2011.
42. Wang, Y., Teng, H.-L., and Huang, Z. Intrinsic migratory properties of cultured Schwann cells based on single-cell migration assay. PLoS One **7,** 1, 2012.
43. Xia, Z., and Triffitt, J.T. A review on macrophage responses to biomaterials. Biomed Mater **1,** R1, 2006.

44. Mikos, A., McIntire, L., Anderson, J., and Babensee, J. Host response to tissue engineered devices. Adv Drug Delivery Rev **33,** 111, 1998.
45. Ghanaati, S., *et al.* Dynamic in vivo biocompatibility of angiogenic peptide amphiphile nanofibers. Biomaterials **30,** 6202, 2009.
46. Hobson, M.I., Green, C.J., and Terenghi, G. VEGF enhances intraneural angiogenesis and improves nerve regeneration after axotomy. J Anat **197,** 591, 2000.
47. Anderson, J.M. Mechanisms of inflammation and infection with implanted devices. Cardiovasc Pathol **2,** 33, 1993.

Address correspondence to:
Matthew V. Tirrell, PhD
Institute for Molecular Engineering
University of Chicago
5747 South Ellis Avenue
Jones Laboratory 222
Chicago, IL 60637

E-mail: mtirrell@uchicago.edu

Received: May 19, 2014
Accepted: December 9, 2014
Online Publication Date: March 9, 2015